A Discontinuous-Galerkin Finite-Element Method for Simulation of Packed Bed Chromatographic Processes

Horsholt, A.; Christiansen, L. H.; Meyer, K.; Huusom, J. K.; Jorgensen, J. B.

Published in:
IFAC-PapersOnLine

Link to article, DOI:
10.1016/j.ifacol.2019.06.086

Publication date:
2019

Document Version
Publisher's PDF, also known as Version of record

Available online at www.sciencedirect.com

ScienceDirect

IFAC PapersOnline CONFERENCE PAPER ARCHIVE

IFAC PapersOnLine 52-1 (2019) 346–351

A Discontinuous-Galerkin Finite-Element Method for Simulation of Packed Bed Chromatographic Processes

A. Hørsholt *, **L.H. Christiansen** *, **K. Meyer** **, **J.K. Huusom** **, **J.B. Jørgensen** *

* *Department of Applied Mathematics and Computer Science & Center for Energy Resources Engineering (CERE), Technical University of Denmark, DK-2800 Kgs. Lyngby, Denmark (e-mails: {aho, lhch, jbo}@dtu.dk)*

** *Process and Systems Engineering Centre (PROSYS), Department of Chemical Engineering, Technical University of Denmark, DK-2800 Kgs. Lyngby, Denmark (e-mails: {krismey, jkh}@kt.dtu.dk)*

Abstract: Packed bed chromatography is an important unit operation for purification of product molecules in biopharmaceutical processes. Packed bed chromatographic processes are modeled as advection-diffusion-reaction partial differential equations. The advection term strongly dominates the diffusion term. Therefore, specialized numerical methods must be used for efficient simulation of packed bed chromatographic processes. In this paper, we use a discontinuous-Galerkin method on finite-elements for spatial discretization and low storage explicit Runge-Kutta (LSERK) methods for numerical solution of the resulting system of differential equations. We study the numerical solution of deterministic and stochastic models of packed bed chromatographic processes. The stochastic model and its corresponding numerical solution constitute the first step toward systematic monitoring, fault detection, and optimal predictive control of chromatographic processes. It is also an essential ingredient in uncertainty quantification for efficient and robust design and operation of chromatographic processes.

Keywords: Chromatography, Mathematical Modeling, Numerical Simulation, Biotechnology.

1. INTRODUCTION

Even though chromatography is a costly separation process, it is extensively used in downstream biopharmaceutical manufacturing (Hong et al., 2018). Consequently, mathematical models for simulation, parameter estimation, design, control, and optimization of chromatographic processes are important. The modeling (Arkell et al., 2018), simulation (Klatt et al., 2000; von Lieres and Andersson, 2010; He et al., 2018; Leweke and von Lieres, 2018; Borg et al., 2013), control (Klatt et al., 2002), and optimization (Püttmann et al., 2013; Holmqvist and Magnusson, 2016; Sellberg, 2018) of chromatographic processes have been extensively studied. Observers for chromatographic procseses have also been studied (Alamir and Corriou, 2003; Corriou and Alamir, 2006; Küpper and Engell, 2006; Küpper et al., 2009; Lemoine-Nava and Engell, 2014). Also many processes such as adsorption possess structural similarities to chromatography, such that the numerical techniques for observers in such processes can be transfered to chromatographic processes (Won and Lee, 2012). In this paper, we use high-order methods for efficient numerical simulation of the advection-diffusion partial differential equation that models chromatographic processes (Hesthaven and Warburton, 2008; Lord et al., 2014). We apply this method to handle stochastic inlet boundary conditions as a first step toward extended and unscented Kalman filters for chromatographic processes. Systematic use of such filters allows for monitoring, prediciton and fault detection of chromatographic processes. The specialized methods, that we use for *simulation* in this paper, are also needed in the extended and unscented Kalman filters for continuous-discrete systems.

1.1 Chromatographic Processes

Chromatography is widely used for separation of peptides and proteins in biopharmaceutical processes (Guichon et al., 2006). Analytically, chromatography is used for separating mixtures into components in order to analyze, identify, purify, quantify, and optimize proceses (Holmqvist and Magnusson, 2016). In production scale, it is used to isolate and purify the compound of interest. Fig. 1 illustrates a chromatographic column. In liquid column chromatography a cylindrical column is packed with a stationary porous material. A continuous flow of liquid with more components are sent to the inlet of the column in a so-called mobile phase. As illustrated in Fig. 1, this creates a flow that moves through the column from the left to the right. The injected liquid contains the mixture

⋆ This work is part of "Model based energy efficient control for the process industries" that is funded by EUDP in the project 64017-05136.

10.1016/j.ifacol.2019.06.086

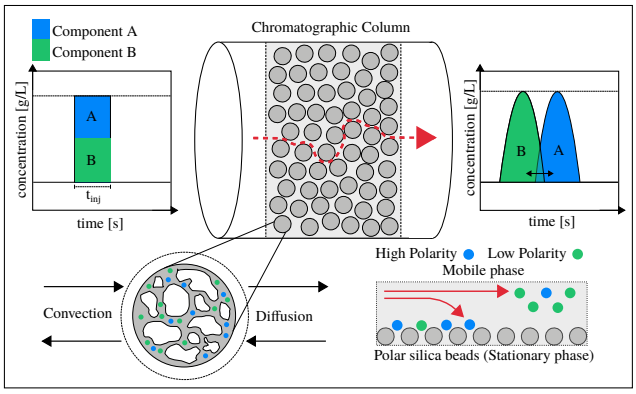

Fig. 1. Conceptual diagram of packed bed chromatographic separation column and the separation principle.

of components. The physical and chemical properties of each component lead to different affinities of the molecules to the mobile and the stationary phase. This difference is used to separate the molecules by having them move along the column at different speeds. Typically, a known solute with a strong affinity to the stationary phase is injected to manipulate pH, polarity or another property that influences the separation of the molecules of interest.

1.2 Motivation

The simulation of multicomponent chromatographic processes under non-linear conditions and reaction kinetics require fast and accurate numerical methods (Javeed et al., 2011; He et al., 2018; Meyer et al., 2018). These processes are typically described by parabolic, non-linear, convection-dominated, coupled partial differential equations (Javeed et al., 2011). Due to the underlying physics, these partial differential equations are advection dominated such that discontinuities in the inputs produces shocks on either side of the elution bands (Ma and Guiochon, 1992). These shocks challenge and cause difficulties for many numerical methods based on finite-difference or finite volume discretization. To mitigate this, we use a high-order nodal discontinuous-Galerkin finite-element (DG-FE) scheme as an accurate and cost efficient simulator (Meyer et al., 2018). We show the h- and p-adaptivity of the scheme by increasing the number of elements for a fixed polynomial order or by increasing the polynomial order for a fixed number of elements (Hesthaven and Warburton, 2008). This validates that the method has the expected high order of accuracy.

Typically, the inlet consist of many complex molecules that are produced by a fermentation in the upstream biopharmaceutical manufacturing process. Often the inlet concentration of these molelcules are not measured, and the concentrations themselves may vary significantly. This significant uncertainty in the inlet concentrations makes it hard to predict the states of a chromatographic process. Efficient state estimators may mitigate this uncertainty by using the available measurements at the outlet. Such estimators require a stochastic model. In this paper, we develop a deterministic model and use it with piecewise constant stochastic inputs. This combination produces a stochastic model that addresses the impact that highly uncertain inlet concentrations have on the outlet concentrations. In a numerical case study, we simulate the deterministic model using the DG-FE simulator with the inlet concentrations being normally distributed and piecewise constant. The results demonstrate the effect that uncertain inlet concentrations have on the simulated states at the outlet and emphasize the need to mitigate this effect by efficient state estimation. This case study also represents a first-step towards observers based on extended and unscented Kalman filter technology.

1.3 Paper Organization

This paper is organized as follows. Section 2 presents the *equilibrium dispersive model* for chromatography that we study in this paper. Section 3 describes the numerical discretization of the model by the DG-FE method. Section 4 presents the numerical results and conclusions are made in Section 5.

2. THE CHROMATOGRAPHIC MODEL

The literature contains a variety of models that describes the behaviour of liquid chromatographic processes inside a separation column. Well known models include the *equilibrium dispersive model*, the *lumped kinetic model*, and the *general rate model* (Guichon et al., 2006). These models are non-linear, convection dominated partial differential equations describing the interaction between chromatographic components inside a separation column, each under varying assumptions. In this work, we consider the *equilibrium dispersive model* (ED). The ED model is derived on six fundamental assumptions (Qamar et al., 2013): 1) The chromatographic process occurring in the separation column is isothermal. 2) The column is radially homogeneous. 3) The stationary phase of the column is packed with a porous material of equally sized spherical particles. 4) The mobile phase is incompressible. 5) The mobile and stationary phase of each component do not interact with each other. 6) There is axial dispersion in the process, which causes band broadening of the concentration profiles.

2.1 The Equilibrium Dispersive Model of Chromatography

The ED model is a partial differential equation of the form (1a) and involves the concentrations of N_c components in the mobile, c_i, and stationary phase, q_i. The transition from mobile to stationary phase is modelled by an equilibrium adsorption isotherm. In the literature, different boundary conditions exist to model almost any configuration of the column (Guichon et al., 2006). A Danckwerts boundary condition is used to model the inlet concentration profile and a zero Neumann condition is given at the outlet (Danckwerts, 1953). Given proper initial conditions, the multi-component ED model is given as

$$\frac{\partial c_i}{\partial t} + F\frac{\partial q_i}{\partial t} = D_i\frac{\partial^2 c_i}{\partial z^2} - v\frac{\partial c_i}{\partial z}, \quad \text{in } \Omega \times (0,T), \tag{1a}$$

$$vc_i - D_i\frac{\partial c_i}{\partial z} = vc_{i,\text{in}}, \quad \text{on } \{0\} \times (0,T), \tag{1b}$$

$$\frac{\partial c_i}{\partial z} = 0, \quad \text{on } L \times (0,T), \tag{1c}$$

$$c_i = c_{i,0}, \quad \text{on } \Omega \times \{0\}, \tag{1d}$$

for all $i = 1, \ldots, N_c$, with total number of components N_c, for a column $\Omega = (0, L)$.

The parameters of (1) is the phase ratio $F = \frac{1-\epsilon_c}{\epsilon_c}$, total porosity of the packing material ϵ_c, interstitial velocity v of the fluid and the ith dispersion coefficient D_i. The dispersion coefficient is related to the number of theoretical plates N_t in the cylinder by Guichon et al. (2006) as $D = \frac{Lv}{2N_t}$.

The ith component is injected into the column with a rectangular pulse of injection time t_{inj} given as

$$c_{i,\text{in}} = \begin{cases} c_{i,f}, & 0 \leq t_{\text{inj}} \leq t, \\ 0, & t_{\text{inj}} < t, \end{cases} \tag{2}$$

with a feed concentration for the ith component $c_{i,f}$.

2.2 The Equilibrium Isotherm

The equilibrium isotherm describes the distribution of a component between the mobile and the stationary phase in the porous media. This implies that in general q_i is a function $q_i = f(c_1, c_2, \ldots, c_i, \ldots, c_{N_c})$ depending on all the components in the chromatographic column. Therefore f is typically a non-linear function that couples the equations in (1).

The competitive Langmuir adsorption isotherm describes a non-linear interaction between components as (Guichon et al., 2006)

$$q_i = \frac{a_i c_i}{1 + \sum_{s=1}^{N_c} b_s c_s}. \tag{3}$$

The linear adsorption isotherm is given as

$$q_i = a_i c_i. \tag{4}$$

For low concentrations the competition between components become almost negligible and (3) typically simplifies to the linear isotherm (4).

2.3 First-Order Equations

To apply the discretization techniques of the DG-FE method, equation (1a) is rewritten as two first order equations (Bassi and Rebay, 1997). Omitting the index i and defining the functions

$$f(c, g(c)) := vc - \sqrt{D} g, \tag{5}$$

$$w(c) := c + Fq(c), \tag{6}$$

equation (1a) takes the form

$$\frac{\partial w}{\partial t}(c, q(c)) = -\frac{\partial}{\partial z}(f(c, g(c)), \tag{7a}$$

$$g(c) = \sqrt{D}\frac{\partial c}{\partial z}. \tag{7b}$$

Solving the equations in (7) is then equivalent to solving (1a).

3. DISCRETIZATION

The model equations (7) are solved using a method-of-lines approach. This procedure allows for a separate discretization of the spatial and temporal variables. The spatial discretization uses a DG-FEM method (Meyer et al., 2018). This discretization recovers a continuous-time-discrete-space system. This semi-discrete system (27) is discretized in time using a low storage, five stage, fourth order explicit Runge-Kutta (LSERK) method (Hesthaven and Warburton, 2008).

3.1 Spatial Discretization

Consider the spatial domain Ω and partition it into N_e non-overlapping elements $z \in [z_l^k, z_r^k] = \Omega_k$, where z_l^k and z_r^k refer to the left and right boundaries on Ω_k. The local solution is approximated on each element, Ω_k, by a polynomial of order $N = N_p - 1$:

$$\begin{bmatrix} w_h^k(z,t) \\ g_h^k(z,t) \end{bmatrix} = \sum_{n=1}^{N_p} \begin{bmatrix} \hat{w}_n^k(t) \\ \hat{g}_n^k(t) \end{bmatrix} \varphi_n(z) = \sum_{i=1}^{N_p} \begin{bmatrix} w_h^k(z_i^k,t) \\ g_h^k(z_i^k,t) \end{bmatrix} l_i^k(z). \tag{8}$$

Here the local solution (w_h^k, g_h^k) may be represented in a modal, $\{\varphi_n\}_{n=1}^{N_p}$, or nodal, $\{l_i^k\}_{i=1}^{N_p}$, basis. In this regard, recall that the Lagrange polynomials, $\{l_i^k\}_{i=1}^{N_p}$, satisfy the interpolation property, $l_i^k(z_j) = \delta_{ij}$ (The Kronecker delta function). Given (8) on each of the N_e elements, the DG-FEM method approximates the global solution, (w, g), by the Nth order piecewise polynomials

$$\begin{bmatrix} w(z,t) \\ g(z,t) \end{bmatrix} \simeq \begin{bmatrix} w_h(z,t) \\ g_h(z,t) \end{bmatrix} = \bigoplus_{k=1}^{N_e} \begin{bmatrix} w_h^k(z,t) \\ g_h^k(z,t) \end{bmatrix}. \tag{9}$$

To determine the approximate solution, (w_h, g_h), the DG-FEM method uses a Galerkin approach. To this end, consider the element-wise, local residuals

$$z \in \Omega^k \ : \mathcal{R}^{(w),k} = \frac{\partial w_h^k}{\partial t} + \frac{\partial f_h^k}{\partial z}, \tag{10a}$$

$$\mathcal{R}^{(g),k} = g_h^k - \sqrt{D}\frac{\partial c_h^k}{\partial z}, \tag{10b}$$

and define the approximation space of piecewise smooth polynomials of order $N = N_p - 1$

$$\mathbb{V}_k^N := \{v \ : v_k \in \mathbb{P}^N(\Omega_k), \forall\, \Omega_k \in \Omega\}, \tag{11}$$

The local, discrete Galerkin approximation to (7) then becomes

$$\int_{\Omega_k} \mathcal{R}_h^{(w),k} \varphi_n(z)\ dz = 0, \tag{12a}$$

$$\int_{\Omega_k} \mathcal{R}_h^{(g),k} \varphi_n(z)\ dz = 0, \tag{12b}$$

where $\{\varphi_n\}_{n=1}^{N_p-1}$ is an appropriate basis for $\mathbb{V}_k^N$. To recover a DG-FEM formulation, the system (12a) is recast to the form (Meyer et al., 2018):

$$\int_{\Omega^k} \frac{\partial w_h^k}{\partial t} l_j^k\ dz + \int_{\Omega^k} \frac{\partial f_h^k}{\partial z} l_j^k\ dz = \oint_{\partial\Omega^k} \hat{n} \cdot (f_h^k - f^*) l_j^k\ dz, \tag{13a}$$

$$\frac{1}{\sqrt{D}} \int_{\Omega^k} g_h^k l_j^k\ dz + \oint_{\partial\Omega^k} \hat{n} \cdot (c_h^k - c^*) l_j^k\ dz = \int_{\Omega^k} \frac{\partial c_h^k}{\partial z} l_j^k\ dz. \tag{13b}$$

Here $c^*(c^-, c^+)$ and $f^*(c^-, c^+, g^-, g^+)$ denote appropriate numerical fluxes, where (-) and (+) refer to interior and exterior interface states of each element, Ω_k. Further, $\partial\Omega_k$ denotes the edges of the kth element and $\hat{n} = (-1, 1)^T$ is the outward pointing unit normal.

3.2 Construction of orthonormal basis functions - $\{\varphi_n\}_{n=1}^{N_p-1}$

Consider the affine mapping $z : [-1, 1] \to \Omega_k$ given by

$$z(\xi) = z_l^k + \frac{1+\xi}{2}\Delta z, \tag{14}$$

where $\Delta z = \Delta z^k = z_r^k - z_l^k$ is the equidistant length of the elements, Ω_k. The orthonormal basis functions, φ_n, are then chosen as the normalized Legendre polynomials

$$\varphi_n(\xi) = \tilde{P}_{n-1}(\xi) = \frac{1}{\sqrt{\frac{2}{2n+1}}} P_{n-1}(\xi), \tag{15}$$

where P_{n-1} are the usual Legendre polynomials. By the map (15), the local, approximate solution is now represented by basis functions defined on the reference element, I. Further, by using the Legendre-Gauss-Lobatto quadrature points on I, the Legendre Vandermonde matrix, $\mathcal{V} \in \mathbb{R}^{N_p \times N_p}$, is well conditioned (Hesthaven and Warburton, 2008). This implies that the the local, element-wise Galerkin operators are given by

$$\mathcal{M}^k = \frac{\Delta z^k}{2} \int_{-1}^{1} l_i^k(\xi) l_j^k(\xi)\, d\xi = \frac{\Delta z^k}{2}\mathcal{M}, \tag{16a}$$

$$\mathcal{S}^k = \int_{-1}^{1} l_i^k(\xi) \frac{dl_j^k}{d\xi}(\xi)\, d\xi = \mathcal{M}\mathcal{D}_\xi, \tag{16b}$$

where $\mathcal{M} = (\mathcal{V}\mathcal{V}^T)^{-1}$. The differentiation matrix is computed by $\mathcal{D}_\xi = \mathcal{V}_\xi \mathcal{V}^{-1}$, where $\mathcal{V}_{\xi,(i,j)} = \frac{d\tilde{P}_j}{d\xi}\Big|_{\xi_i}$ is the gradient of the Vandermonde matrix. Note that the affine mapping allows for exact evaluation of the integrals (16) without the use of quadrature rules (Hesthaven and Warburton, 2008). Now, by substitution of the nodal expansion (8) and the operators (16) into (13), the semi-discrete form becomes

$$\mathcal{M}^k \frac{\partial w_h^k}{\partial t} + \mathcal{S}^k f_h^k = \mathcal{E}\left[\hat{n}\cdot(f_h^k - f^*)\right]_{z_l^k}^{z_r^k}, \tag{17a}$$

$$\mathcal{M}^k g_h^k = \sqrt{D}\mathcal{S}^k c_h^k - \sqrt{D}\mathcal{E}\left[\hat{n}\cdot(c_h^k - c^*)\right]_{z_l^k}^{z_r^k}. \tag{17b}$$

Here the local operator $\mathcal{E}$ extracts the surface term and $\mathcal{E} = (e_1, e_{N_p})$, where e_i is a N_p size vector with value 1 at position i. The final semi-discrete form is recovered from (17)

$$\frac{\partial w_h^k}{\partial t} = -\frac{2}{\Delta z}\mathcal{D}_\xi h_h^k + \frac{2}{\Delta z}\mathcal{L}\left[\hat{n}\cdot(f_h^k - f^*)\right]_{z_l^k}^{z_r^k}, \tag{18a}$$

$$g_h^k = \frac{2\sqrt{D}}{\Delta z}\mathcal{D}_\xi c_h^k - \frac{2\sqrt{D}}{\Delta z}\mathcal{L}\left[\hat{n}\cdot(c_h^k - c^*)\right]_{z_l^k}^{z_r^k}, \tag{18b}$$

where $(w_h^k, g_h^k, f_h^k) \in \mathbb{R}^{N_p}$ is the nodal coefficients on each element, Ω_k, and $\mathcal{L} := {\mathcal{M}^k}^{-1}\mathcal{E}$ is the lifting matrix.

3.3 Numerical Flux Functions

To capture the physical phenomena of the model (1), the following specifies appropriate numerical fluxes, (c^*, g^*, f^*). The fluxes may be approximated by a variety of options (Javeed et al., 2011). The following choices are based on considerations presented in Meyer et al. (2018). Given the diffusive nature of band broadening, c^* is approximated on all element boundaries by a central flux

$$c^* = \frac{c^- + c^+}{2}. \tag{19}$$

The field differences on each element interface are then

$$\hat{n}\cdot(c_h^k - c^*) = \hat{n}\cdot(c^- - c^+). \tag{20}$$

Given the definition of f in (5), it is reasonable to consider f^* as the sum of a convective and diffusive term

$$f^* = f^*_{\text{conv}}(c^-, c^+) + f^*_{\text{diff}}(g^-, g^+). \tag{21}$$

The convective term is approximated by an upwind flux and the diffusive term by a central flux on all interfaces, except at the left boundary

$$f^* = \frac{v}{2}(c^- + c^+ + \hat{n}\cdot(c^- + c^+)) + \sqrt{D}\frac{g^- + g^+}{2}. \tag{22}$$

The field differences on each element interface, excluding the left boundary, is given by

$$\hat{n}\cdot(f_h^k - f^*) = \hat{n}\cdot\frac{\left(v(c^- - c^+) - \sqrt{D}(g^- - g^+)\right)}{2} - \frac{v(c^- - c^+)}{2}. \tag{23}$$

On the remaining left most interface, the flux is specified as a central flux to ease the implementation of the Robin boundary condition, thereby giving rise to the field difference

$$\hat{n}\cdot(f_h^k - f^*) = \hat{n}\cdot(f^- - f^+). \tag{24}$$

3.4 Imposing the Boundary Conditions

The DG-FEM method allows for a practical implementation of the boundary conditions, which is done weakly by defining the exterior ghost states (c^+, g^+) at the left and right most boundary of Ω. The Robin boundary condition (1b) at the inlet is implemented by requiring that

$$c_h^+ = c_h^-, \quad f_h^+ = -f_h^- + 2vc_{i,\text{in}}. \tag{25}$$

Similarly, the Neumann condition (1c) at the outlet is enforced by the requirement that

$$c_h^+ = c_h^-, \quad g_h^+ = -g_h^-. \tag{26}$$

3.5 Forward Time Integration

To advance the semi-discrete form (18) in time, the DG-FEM approach uses the chain-rule on $\frac{\partial q_i}{\partial t}$ in (1a) to obtain

$$\frac{\partial c^k}{\partial t} = \left(\mathcal{I} + F\frac{\partial q^k}{\partial c^k}\right)^{-1}\frac{\partial w^k}{\partial t}. \tag{27}$$

Now, c^k and w^k correspond to row vectors in $\mathbb{R}^{N_p N_c}$ that contain the stacked nodal values (c_h^k, w_h^k) for each component i on each element. $\frac{\partial q^k}{\partial c^k}$ is the Jacobian in $\mathbb{R}^{N_p N_c \times N_p N_c}$ of the associated equilibrium isotherm evaluated in the corresponding nodal values of c^k as diagonals in the Jacobian. $\mathcal{I}$ is the identity matrix. The right hand side is evaluated at every element Ω_k for every component i to produce a set of ODEs that are solved using an LSERK method.

4. NUMERICAL CASE STUDY

To demonstrate the capabilities of the DG-FE method, the following considers two case studies. To verify the DG-FEM scheme, the first study performs a convergence test for the linear isotherm (4) that compares the error between the known solution given by van Genuchten (1981) and the

Table 1. Simulation parameters for linear case study.

Parameters	Symbol	Value	Metric
Column Length	L	1	[cm]
Porosity	ϵ	0.5	-
Interstitial velocity	v	1	[cm/min]
Theoretical plates	N_t	300	-
Henry's constant	a	1	-
Initial concentration	c_0	0	g/L
Feed concentration	c_f	1	g/L

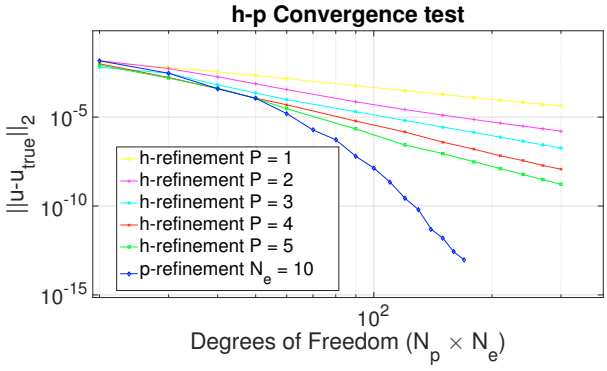

Fig. 2. h- and p- adaptivity of the one component, linear isotherm problem.

computed DG-FEM solution. To represent the inherent uncertainty of the chromatographic process, the second study performs a stochastic simulation of the non-linear Langmuir isotherm with a piecewise normally distributed inlet concentration noise and a noisy initial concentration.

4.1 Case I: One component, linear isotherm

This case study demonstrates numerical convergence of the DG-FEM scheme by verifying the $h\backslash p$-adaptivity of the error, which is defined by the difference between the numerical and analytical solution, i.e., $e_a = c - c_a$. Table 1 lists the simulation parameters. The injection is a rectangular pulse of $c_f = 1$ of time $t_{\text{inj}} = 1$. The final simulation time is $t_f = 4$.

The error is measured in the $L^2(\Omega)$ norm as

$$||e_a||_{\Omega,h} = \sum_{k=1}^{N_e} ||e_a||_{\Omega_k} = \sum_{k=1}^{N_e} \sqrt{(e_a^k)^T \frac{\Delta z^k}{2} \mathcal{M} e_a^k}, \qquad (28)$$

which is similar to the standard 2-norm. Figure 2 compares the results of h- and p- adaptivity. These are two complementary refinement techniques. In h-adaptivity, the polynomial order, N, is constant and the mesh is adjusted. In p-adaptivity, N_e is kept constant while the polynomial order is increased on each element. In particular, p- adaptivity proves superior to h- adaptivity in terms of DOFs and accuracy.

4.2 Case II: Two components, stochastic, non-linear isotherm

This case study investigates the effect of introducing process noise on the inlet concentration of the column. The inlet concentration $c_{i,f}$ is perturbed

$$c_{i,\text{in}}^{\Delta w} = \begin{cases} c_{i,f} + \Delta w, & 0 \leq t_{\text{inj}} \leq t, \\ \Delta w^c, & t_{\text{inj}} < t, \end{cases} \qquad (29)$$

Table 2. Simulation parameters for the non-linear, stochastic case study. The uncertain initial states in the column are sampled as $\Delta v \sim \mathcal{N}(0,1)$ for positively constrained noises Δv_1^c and Δv_2^c .

Parameters	Symbol	Value	Metric
Column Length	L	1	[cm]
Porosity	ϵ	0.4	-
Interstitial velocity	v	0.1	[cm/min]
Theoretical plates	N_t	3000	-
Henry's constant	a_1, a_2	0.05, 10	-
Constants	b_1, b_2	0.005, 1	L/mol
Initial concentration	$c_{1,0}^{\Delta v}, c_{2,0}^{\Delta v}$	$\Delta v_1^c, \Delta v_2^c$	g/L
Feed concentration	$c_{1,f}, c_{2,f}$	10, 10	g/L

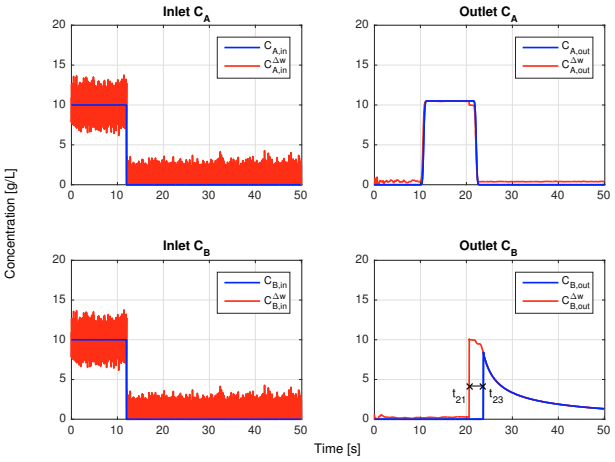

Fig. 3. Comparison of inlet and outlet concentrations (c_1, c_2) for the deterministic and stochastic model.

Table 3. The RMSE calculated between deterministic and stochastic band profile at different times t_j.

RMSE	t_1	t_5	t_7	t_{12}	t_{15}	t_{20}	t_{23}
c_1	14.32	10.38	7.94	1.34	2.36	8.83	13.65
c_2	12.45	17.09	20.41	27.47	32.70	41.27	10.18

and the piecewise noise is sampled from $\Delta w \sim \mathcal{N}(0,1)$, where $\Delta w^c = \Delta w > 0$. Table 2 lists the simulation parameters. The injection profiles are noisy, rectangular pulses of time $t_{\text{inj}} = 12$ with final simulation time $t_f = 50$. Figure 3 compares the noisy, inlet concentrations of component 1 and 2 with the respective, predicted states at the outlet. Compared to the deterministic case, the stochastic model results show a significant variation in the predicted states at the column outlet. Table 3 displays the RMSE values that are calculated based on the deterministic and stochastic band profiles for times t_j. As Table 3 shows, the stochastic band profile for c_1 indicates a varying deviation. The stochastic band profile for c_2 shows large variations until $t = 23$, before it collapses and dissipates complementary to the deterministic prediction. In particular, a large gap between both simulations for c_2 occurs at t_{21} to t_{23}. As a result, the area $A_{c_2,\text{out}}^{\Delta w}$ and $A_{c_2,\text{out}}$ is 7.75×10^4 and 3.73×10^4 deviates significantly.

5. CONCLUSION

This paper presents a high-order DG-FE method for efficient and accurate simulation of chromatographic processes that can be described by the ED model. This is motivated by the observation that high-order methods should be considered when simulating convection-dominated nonlinear partial differential equations such as (1). As the main contribution, this paper considers the effects of uncertainties in the inlet concentrations. The stochastic simulation demonstrates significant deviations between the deterministic and stochastic states and outlet concentrations. The stochastic chromatographic simulation model is a first step towards observers based on extended and unscented Kalman filter technology.

REFERENCES

Alamir, M. and Corriou, J.P. (2003). Nonlinear receding-horizon state estimation for dispersive adsorption columns with nonlinear isotherm. *Journal of Process Control*, 13, 517–523.

Arkell, K., Breil, M.P., Frederiksen, S.S., and Nilsson, B. (2018). Mechanistic modeling of reversed-phase chromatography of insulins within the temperature range 10-40°C. *ACS Omega*, 3, 1946–1954.

Bassi, F. and Rebay, S. (1997). A high-order accurate discontinuous finite element method for numerical solution of the compressible navier-stokes equations. *Journal of Computational Physics*, 131(2).

Borg, N., Westerberg, K., Andersson, N., von Lieres, E., and Nilsson, B. (2013). Effects of uncertainties in experimental conditions on the estimation of adsorption model parameters in preparative chromatography. *Computers & Chemical Engineering*, 55, 148–157.

Corriou, J.P. and Alamir, M. (2006). A hybrid nonlinear state observer for concentration profiles reconstruction in nonlinear simulated moving bed. *Journal of Process Control*, 16, 345–353.

Danckwerts, P. (1953). Continuous flow systems. distribution of residence times. *Chemical Engineering Science*, 2, 1–13.

Guichon, G., Felinger, A., Shirazi, D., and Katti, A. (2006). *Fundamentals of Preparative and Nonlinear Chromatography*. Elsevier, 2nd ed edition.

He, Q.L., Leweke, S., and von Lieres, E. (2018). Efficient numerical simulation of simulated moving bed chromatography with a single-column solver. *Computers & Chemical Engineering*, 111, 183–198.

Hesthaven, J. and Warburton, T. (2008). *Discontinuous nodal Galerkin methods algorithms analysis and applications*. Springer.

Holmqvist, A. and Magnusson, F. (2016). Open-loop optimal control of batch chromatographic separation processes using direct collocation. *Journal of Process Control*, 46, 55–74.

Hong, M.S., Severson, K.A., Jiang, M., Lu, A.E., Love, J.C., and Braatz, R.D. (2018). Challenges and opportunities in biopharmaceutical manufacturing control. *Computers & Chemical Engineering*, 110, 106–114.

Javeed, S., Shamsul, Q., Andreas, S., and Warnecke, G. (2011). A discontinuous Galerkin method to solve chromatographic models. *Journal of Chromatography A*, 1218(40), 7137 – 7146.

Klatt, K.U., Dünnebier, G., and Engell, S. (2000). Modeling and computational efficient simulation of chromatographic separation processes. *Mathematics and Computers in Simulation*, 53, 449–455.

Klatt, K.U., Hanish, F., and Dünnebier, G. (2002). Model-based control of a simulated moving bed chromatographic process for the separation of fructose and glucose. *Journal of Process Control*, 12, 203–219.

Küpper, A., Diehl, M., Schlöder, J.P., Bock, H.G., and Engell, S. (2009). Efficient moving horizon state and parameter estimation for SMB processes. *Journal of Process Control*, 19, 785–802.

Küpper, A. and Engell, S. (2006). Parameter and state estimation in chromatographic SMB processes with individual columns and nonlinear adsorption isotherms. In *International Symposium on Advanced Control of Chemical Processes (ADCHEM)*, 611–616. Gramado, Brazil.

Lemoine-Nava, R. and Engell, S. (2014). Individual column state and parameter estimation in the simulated moving bed process: an optimization-based method. In *Proceedings of the 19th IFAC World Congress*, 9376–9381. Cape Town, South Africa.

Leweke, S. and von Lieres, E. (2018). Chromatography Analysis and Design Toolkit (CADET). *Computers & Chemical Engineering*, 113, 274–294.

Lord, G.J., Powell, C.E., and Shardlow, T. (2014). *An Introduction to Computational Stochastic PDEs*. Cambridge University Press, New York, NY, USA.

Ma, Z. and Guiochon, G. (1992). Shock layer thickness in the case of wide bands of single components and binary mixtures in non-linear liquid chromatography. *Journal of Chromatography A*, 609(1), 19 – 33.

Meyer, K., Huusom, J.K., and Abildskov, J. (2018). High-order approximation of chromatographic models using a nodal discontinuous Galerkin approach. *Computers & Chemical Engineering*, 109, 68 – 76.

Püttmann, A., Schnittert, S., Naumann, U., and von Lieres, E. (2013). Fast and accurate parameter sensitivities for the general rate model of column liquid chromatography. *Computers & Chemical Engineering*, 56, 46–57.

Qamar, S., Abbasi, J.N., Javeed, S., Shah, M., Khan, F.U., and Seidel-Morgenstern, A. (2013). Analytical solutions and moment analysis of chromatographic models for rectangular pulse injections. *Journal of Chromatography A*, 1315, 92 – 106.

Sellberg, A. (2018). *Open-Loop Optimal Control of Chromatographic Separation Processes*. Ph.D. thesis, Department of Chemical Engineering, Lund University, Lund, Sweden.

van Genuchten, M.T. (1981). Analytical solutions for chemical transport with simultaneous adsorption, zero-order production and first-order decay. *Journal of Hydrology*, 49(3), 213 – 233.

von Lieres, E. and Andersson, J. (2010). A fast and accurate solver for the gerenal rate model of column liquid chromatography. *Computers & Chemical Engineering*, 34, 1180–1191.

Won, W. and Lee, K.S. (2012). Nonlinear observer with adaptive grid allocation for a fixed-bed adsorption process. *Computers & Chemical Engineering*, 46, 69–77.